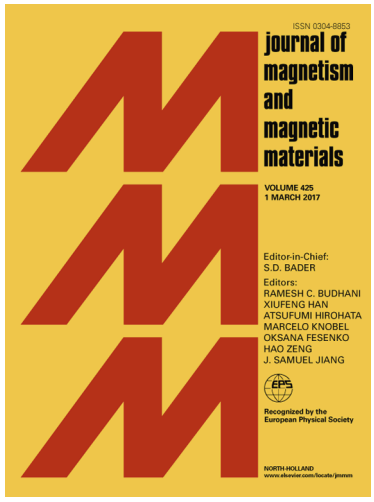

Research articles

Detection of magnetic moment in thin films with a home-made vibrating sample magnetometer

D. Jordán, D. González-Chávez, D. Laura, L.M. León Hilario, E. Monteblanco, A. Gutarra, L. Avilés-Félix

PII: S0304-8853(17)33341-3
DOI: https://doi.org/10.1016/j.jmmm.2018.01.088
Reference: MAGMA 63666

To appear in: *Journal of Magnetism and Magnetic Materials*

Received Date: 24 October 2017
Revised Date: 1 January 2018
Accepted Date: 27 January 2018

Please cite this article as: D. Jordán, D. González-Chávez, D. Laura, L.M. León Hilario, E. Monteblanco, A. Gutarra, L. Avilés-Félix, Detection of magnetic moment in thin films with a home-made vibrating sample magnetometer, *Journal of Magnetism and Magnetic Materials* (2018), doi: https://doi.org/10.1016/j.jmmm.2018.01.088

Detection of magnetic moment in thin films with a home-made vibrating sample magnetometer

D. Jordán[a,1], D. González-Chávez[a,b], D. Laura[a], L. M. León Hilario[a], E. Monteblanco[a,c], A. Gutarra[a], L. Avilés-Félix[a,d,2]

[a] *Laboratorio de Materiales Nanoestructurados, Facultad de Ciencias, Universidad Nacional de Ingeniería, Avenida Túpac Amaru 210, Rímac 025, Lima Perú.*
[b] *Centro Brasileiro de Pesquisas Físicas, 22290-180 Rio de Janeiro, RJ, Brazil.*
[c] *Département P2M Nanomagnétisme et Electronique de Spin, Institut Jean Lamour, Université de Lorraine, Boulevard des Aiguillettes, Villers-lés-Nancy, Nancy, France.*
[d] *Centro Atómico Bariloche-Instituto Balseiro, Avenida Ezequiel Bustillo 9500, San Carlos de Bariloche, Rio Negro 8400, Argentina.*

Abstract

This paper explores the optimization of an array of pick-up coils in a home-made vibrating sample magnetometer for the detection of magnetic moment in thin films. Sensitivity function of a 4-coils Mallinson configuration was numerically studied for the determination of the physical dimensions that enhance the sensitivity of the magnetometer. By performing numerical simulations using the Biot-Savart law combined with the principle of reciprocity we were able to determine the maximum values of sensitivity and the influence of the separation of the coils on the sensitivity function. After the optimization of the pick-up coils, the vibrating sample magnetometer was able to detect the magnetic moment of a 100 nm-thickness $Fe_{19}Ni_{81}$ magnetic thin film along and perpendicular to the in-plane anisotropy easy axis. The implemented vibrating sample magnetometer is able to detect changes in the magnetic moment of $\sim 2 \times 10^{-4}$ emu.

Keywords: Vibrating sample magnetometer, magnetometry, principle of reciprocity, Sensitivity function, magnetic thin films.

[1] Current address:Centro Atómico Bariloche-Instituto Balseiro, Avenida Ezequiel Bustillo 9500, San Carlos de Bariloche, Rio Negro 8400, Argentina
[2] Corresponding author:lavilesf@gmail.com

1. Introduction

The measurement of magnetic moments using a Vibrating Sample Magnetometer (VSM) is based on the Faraday's law. The electromagnetic induction in an array of coils caused by the controlled motion of a magnetic sample in the vicinity of the coils gives quantitative information related to the magnetic moment of a sample [1]. This mechanism of magnetic moment detection is known as inductive detection and its sensitivity and performance is strongly related to the pick-up coil configuration, physical dimensions and cross section of the coils. Since the fabrication of the VSM in 1959 by Simon Foner, several authors reported relevant aspects of this type of magnetometer, such as theoretical and numerical calculation of the induced electromotive force [2], study and determination of the sensitivity function [3] and increase of the sensitivity [4]. In this frame, the works of Zieba *et al.* [3] and Mallinson [5] highlight the important role of the physical dimensions and characteristics of the pick-up coils on the sensitivity function of the magnetometer. Mallinson published the first work on the determination of the optimal dimensions of the 4-coils configuration using the principle of reciprocity in electromagnetism [5]. This principle is a consequence of the mutual inductance between two coils and states that the mutual flux threading two coils is independent of which one carries the current. On the other hand, Zieba *et al.* [3] performed approximations of the sensitivity function for axial and transversal coil configurations using spherical harmonic expansions. Their results allowed to quantitatively compare the sensitivity function for different coil arrangements that employ even number of coils and also to study the influence of the sample geometry on the output signal of the coils.

These works were the foundations for the implementation of low cost homemade vibrating sample magnetometers [6, 7, 8, 9], particularly at undergraduate level in physics. However, it is important to notice that most of these works focused their results on the construction and calibration of the VSM for the detection of samples with high magnetic signal. There are only a few papers that focused their attention into the design and optimization of the physical

dimensions of the pick-up coils in order to enhance the sensitivity function of the magnetometer, that allows to detect magnetization in thin films or samples with low magnetic signal. This work discusses the influence of the coil dimensions on the sensitivity function through numerical simulations using the Biot-Savart law combined with the principle of reciprocity.

2. Experimental details

A schematic of the implemented VSM is shown in Fig. 1. The oscillatory motion of the magnetic sample is controlled by a loudspeaker of 30 W of power. Samples were placed at the end of a glass rod of 5 mm-diameter attached to the loudspeaker membrane. Pick-up coils were fabricated using copper wire AWG-42. Each coil has approximately 6500 turns and was compensated by measuring the induced voltage produced by an alternating magnetic field. The number of turns per coil was determined through the induced voltage; each coil induces the same voltage for a fixed value of alternating magnetic field. A Stanford Research SR-830 lock-in amplifier was used not only for the detection and amplification of the output voltage in the coils, but also to supply the reference signal to the loudspeaker. A KEPCO BOP 50-8 ML power source that supplies a CENCO electromagnet produces an external magnetic field of up to 2000 Oe. The magnetic field was detected and measured by a transversal Hall probe connected to a magnetic transducer GLOBALMAG model TMAG-V2 with an analog output. Fig 1b) shows an image of the sample zone indicating the position of the pick-up coils and the placement of the sample.

The data collection of the VSM was performed using the programming language Python[10] to control the data communication through a GPIB-Ethernet interface. Numerical simulations for the determination of the sensitivity function of the magnetometer were also performed using Python.

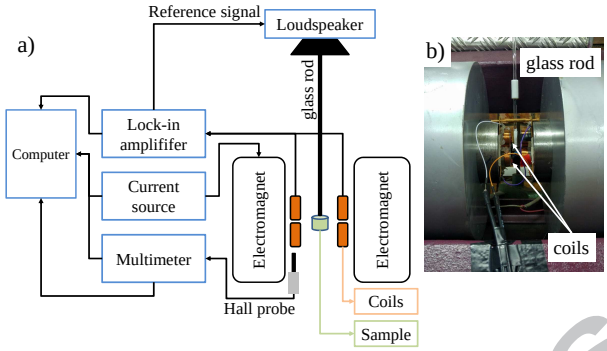

Figure 1: (a) Block diagram of the home-made VSM (b) Image of the vibrating sample magnetometer indicating the pick-up coils placement and the glass rod that supports the magnetic sample.

3. Results and Dicussions

Numerical simulations of the sensitivity function are based on the principle of reciprocity and the Biot-Savart law. In order to determine the output voltage V_{ind} of the pick-up coils, it is necessary to calculate the integral of flux change $\frac{d\Phi}{dt}$ generated by the movement of the magnetic sample, according to Faraday's law: $V_{ind} = -\frac{d\Phi}{dt}$. On the other hand, by applying the principle of reciprocity, it is possible to estimate the flux inside each coil in our coils-sample system, through the relation $\vec{B} \cdot \vec{\mu} = I\Phi$. In this relation $\vec{\mu}$ is the magnetic moment of the sample, I is the current passing through the coils and $\vec{B}$ is the magnetic field at the position of the magnetic moment. According to this, we deduced that the induced voltage in the pick-up coils depends on the magnetic moment of the sample μ, the sensitivity function G($\vec{r}$) and the velocity of the sample, as shown in Eq. 1[3, 11]:

$$V_{ind} = -\frac{d\Phi}{dz}\frac{dz}{dt} = grad\left(\frac{\vec{B}(\vec{r}) \cdot \vec{\mu}}{I}\right) \cdot \vec{v}(t) = \mu G(\vec{r}) v(t) \ , \qquad (1)$$

where $G(\vec{r}) = grad\left(\frac{\vec{B}(\vec{r})\cdot\hat{e}_{\vec{\mu}}}{I}\right)\cdot\hat{e}_{\vec{v}}$ is the sensitivity function. We considered in Eq. 1 that z is the oscillation direction of the magnetic sample and $v(t) = A\omega\cos(\omega t)$ is the velocity of the sample. We also observed in Eq. 1 that the induced voltage is proportional to the amplitude and frequency of the oscillatory motion of the magnetic sample. A coordinate system describing the relative orientation between the axis of the coils and the oscillation direction of the sample in our magnetometer is shown in Fig. 2a). Using the coordinate system shown in Fig. 2b) where $\hat{e}_{\vec{\mu}} \parallel \hat{y}$ and $\hat{e}_{\vec{v}} \parallel \hat{z}$, the sensitivity function $G(\vec{r})$ can be reduced to the following:

$$G(\vec{r}) = \frac{\partial B_y(\vec{r})}{\partial z}. \tag{2}$$

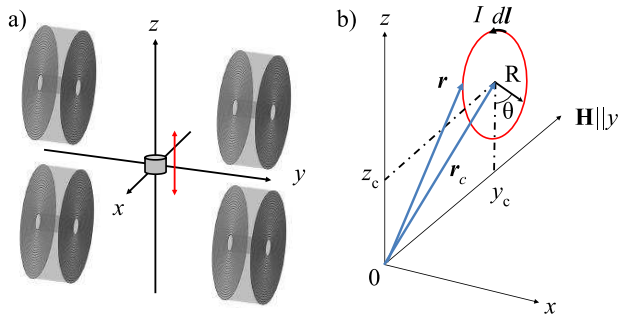

Figure 2: (a) Coordinate system that describe the relative orientation between the axis of the coils and the oscillation direction of the sample. The magnetic field is applied along y axis and the movement of the sample is along z axis (vertical arrow). (b) Coordinate system and vectors used for the calculation of the magnetic field at the sample position. Vertical and horizontal separation of the center of the coils with respect to the z and y axis are z_c and y_c respectively.

To calculate the sensitivity function of the Mallinson configuration in our magnetometer we used the Biot-Savart relation:

$$\vec{B} = \frac{1}{c} \oint \frac{I d\vec{l} \times \vec{r}}{r^3}, \tag{3}$$

where I is the current passing in each coil, $d\vec{l}$ is the differential vector on the contour of the loops and $\vec{r}$ is the displacement vector from the wire element to the origin of the coordinate system. To compute the magnetic field, we considered that the vector from the origin (sample's position) to the center of the coil has coordinates $\vec{r}_c = (0, y_c, z_c)$ and the vector that determines the external contour of the coil (in the xz plane) is $\vec{r}_e = (R\sin\theta, 0, -R\cos\theta)$. According to this, the vector that describes the position of a point in the contour of the loops is given by $\vec{r} = -(\vec{r}_c + \vec{r}_e) = -(R\sin\theta, y_c, z_c - R\cos\theta)$. The differential vector $d\vec{l}$, was calculated taking the derivative of $\vec{r}_e$ with respect to θ: $d\vec{l} = (R\cos\theta, 0, R\sin\theta)\, d\theta$. Therefore, the cross product of equation 3 is given by $d\vec{l} \times \vec{r} = (y_c R\sin\theta, z_c R\cos\theta - R^2, -y_c R\cos\theta)\, d\theta$. As a result, the integral of Eq. 3 results in an angular integral from 0 to 2π:

$$\vec{B} = \frac{I}{c} \int_0^{2\pi} \frac{(y_c R\sin\theta, z_c R\cos\theta - R^2, -y_c R\cos\theta)}{(R^2 + y_c^2 + z_c^2 - 2z_c R\cos\theta)^{3/2}} d\theta\,. \tag{4}$$

According to Eq. 2, to determine the sensitivity function it is necessary to calculate the y-component of the magnetic field $\vec{B}$:

$$B_y = \frac{I}{c} \int_0^{2\pi} \frac{z_c R\cos\theta - R^2}{(R^2 + y_c^2 + z_c^2 - 2z_c R cos\theta)^{3/2}} d\theta\,. \tag{5}$$

In order to compute the sensitivity of the whole coil, we must add the contribution of all loops. Therefore, a more generalized expression for the sensitivity function in each coil is given by the following expression:

$$G(\vec{r}) = \frac{I}{c} \sum_{m=0}^{n_s} \sum_{n=0}^{n_l} \frac{\partial}{\partial z_c} \int_0^{2\pi} \frac{z_c(R_{int} + md)\cos\theta - (R_{int} + md)^2}{[(R_{int} + md)^2 + (y_c + nd)^2 + z_c^2 - 2z_c(R_{int} + id) cos\theta]^{3/2}} d\theta\,. \tag{6}$$

where we have considered d as the diameter of the wire, n_l is the number of loops to make a solenoid and n_s is the number of solenoid shells that make up the entire sensing coil. From the previous equation we notice that the first

sum builds the coil axially, such that $n_l \times d$ equals its length. The second sum varies the radius in the integral such that it starts at r_{int} and ends with $r_{int} + n_s \times d = R_{ext}$. It is important to notice that the integration limits depend on the coil that is being considered. Mallinson's geometry requires that the four balanced coils must be wounded in series opposition [5], in order to obtain a maximum output signal and to reduce the electrical response of the coils to the magnet or to external signals. In our model, the integration limits will be determined by the current direction in each coil.

In order to estimate the derivative of B_y with respect to z we calculated the integral in Eq. 6 evaluated in $z = z_c \pm \delta z$ to numerically estimate the sensitivity function according to the following expression:

$$G(\vec{r}) = \frac{\partial B_y(\vec{r})}{\partial z} \approx \frac{B_{y+} - B_{y-}}{2\delta z}\,, \tag{7}$$

where B_{y+} and B_{y-} correspond to the integral evaluated in $z_c + \delta z$ and $z_c - \delta z$ respectively. Numerical calculation of the sensitivity function allow us to obtain $G(\vec{r})$ for different Mallinson configurations. This analysis will help us to determine not only the required dimensions of the coils but also the influence of the relative position between the coils, external and internal radius on the sensitivity function of the magnetometer. The Python code used and a detail description of the calculation of the sensitivity function is given in the supplementary file of the manuscript.

3a) *Influence of the y- and z-axis separation of the coils.*- Numerical calculation of equations 6 and 7 allow us to determine the maximum values of the sensitivity as a function of the $y-$ and $z-$separation of the coils. Fig. 3 shows the influence of the separation of the coils in both axis labeled as y_c and z_c, according to the coordinate system shown in Fig. 2b). It is important to notice that the $y-$axis separation is limited by the gap that determines the sample's position, around 1 cm in most of the cases. For the calculations we have considered an external radius of the coils of 1.5 cm, that limits the vertical separation

(z_c). On the one hand, in Fig. 3a) the sensitivity function of the coils configuration is plotted as a function of the horizontal separation y_c for different values of z_c. As expected, in the case of a zero vertical gap between the coils, corresponding to a value of $z_c = 1.5$ cm, there is a notable increase of the sensitivity function, that rapidly decreases as the value of z_c increases.

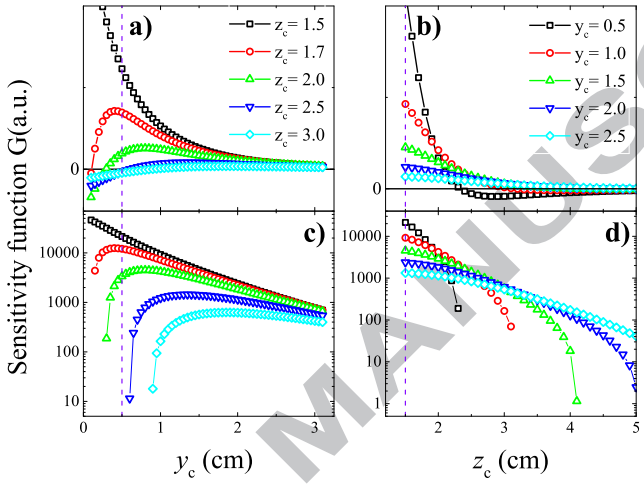

Figure 3: (a) Sensitivity as a function of the the y-axis separation of the coils y_c for different values of z_c. The vertical dashed line indicates the limit of the region in the y-axis where the sample is placed. Units of sensitivity function are Gauss/cm. (b) Sensitivity as a function of the the z-axis separation of the coils z_c for different values of y_c. The vertical dashed line indicates that the vertical gap between the coils is zero, due to its external radius $z_c = 1.5$ cm. (c) Log-linear plot of $G(r)$ as a function of the y-axis separation for different values of z_c. (d) Log-linear plot of $G(r)$ as a function of the z-axis separation for different values of y_c.

On the other hand, the dependence of the vertical separation on the sensitivity function of the coils (Fig. 3b)) also shows an increase as we decrease the separation of the center of the coils and the y axis. This result verifies that a higher sensitivity of the function can be achieved as we approach the pairs of coils in the y axis. Fig. 3a) and 3b) also show that the sensitivity function can also take negative values. This behavior of the sensitivity function is a consequence of the spacial distribution of the stray field of the magnetic sample, that in some cases induces a change of the current sense in the coils. Figures 3c) and

3d), that show the sensitivity function in a log-linear plot, evidenced that the dipole decays of the sensitivity function changes through 4 orders of magnitude for y-axis separation of the coils below 1 cm for different values of z_c. However, for the selected values of y_c, we appreciate that the sensitivity function does not change in the same way for z-axis separation, due to $G(r)$ rapidly goes to zero as shown in Fig. 3d). Our results agree with previous calculations performed by other authors that also show the same behavior of the sensitivity function [12]. More detailed calculations performed by our group indicate that there is a region near the coils where the $G(r)$ can take negative values. A report of these results will be published shortly.

3b) *Influence of the internal and external radius on the sensitivity function.-* Numerical simulations varying the internal and external radius of the coils were also performed. As it was mentioned above, the internal radius parameter r_{int} was included into the calculation of the sensitivity function in Eq. 6. The detail description of the calculation of the sensitivity function is given in the supplementary file. Fig. 4 shows the sensitivity as a function of the external radius of the coils for different values of internal radius r_{int}. Simulations revealed that the sensitivity function increases up to a maximum value of $G(\vec{r})$ around R_{ext} = 3.5 cm. This maximum value of the sensitivity can be explained by the $1/R^2$ dependence of the integral in Eq 5.

As expected, we also observed in Fig. 4 that for smaller values of the external radius, the sensitivity function increases as we decrease the internal radius.

According to the results on the influence of the internal and external radius of the coils and also of the vertical and horizontal separation on the sensitivity function it is possible to determine the optimal dimensions and placement of the pick-up coils for our magnetometer. Having into consideration the dimensions of our electromagnet and the gap between the poles we chose a region in Fig. 4 (indicated by vertical lines) with adequate values for r_{int} and R_{ext} without reducing the sensitivity considerably. We set the dimensions and relative placement of the pick-up coils to y_c = 1 cm, r_{int} = 1 cm and $R_{ext} = z_c$ = 1.5 cm.

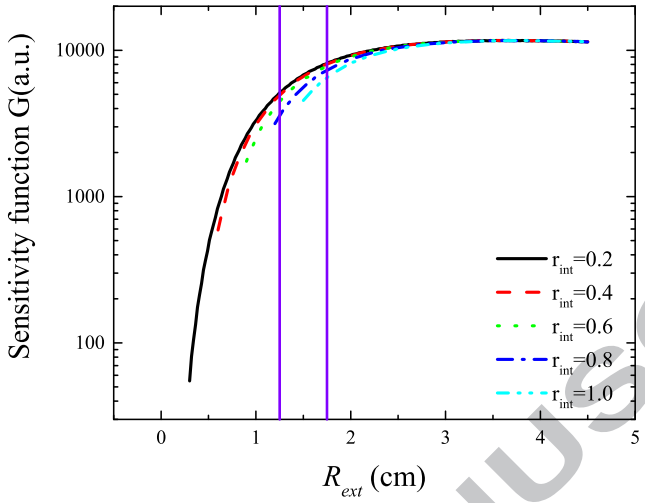

Figure 4: Sensitivity as a function of the the external radius for different values of the internal radius r_i of the pick-up coils.

The coils were fabricated avoiding wire breaks during wounding. Considering these dimensions for our pick-up coils, a rough estimation of the induced signal can be obtained. A sample with a magnetic moment of 1×10^{-4} emu (or 1×10^{-7} A m^2) will generate a magnetic field at the vicinity of the coils (placed at $y_c = 1$ cm) of ~ 0.1 μT (according to the Biot-Savart law). This value multiplied by the number of turns, the vibration frequency and integrated over the surface of the coils ($r_{int} = 1$ cm) gives and induced voltage of 20 μV. This estimated induced voltage agrees with the induced signal detected by our coils in the experiments performed during the optimization of our vibrating sample magnetometer: 0.1 - 10 μV.

3c) *Hysteresis loops of $Fe_{19}Ni_{81}$ thin films.*- The magnetic moment of the sample was measured using a time constant of $\tau = 100$ ms, an oscillation frequency of $f = 95$ Hz and a supplied voltage to the loudspeaker of $V = 1$ V_{rms}. The required time to complete a magnetic field cycle (starting from $+H$ to -H and then to $+H$) is around 50 minutes.

Figure 5a) shows the magnetization measurements with the external mag-

netic field applied along the in-plane easy axis of a Si(100)//FeNi(100 nm) thin film. The dimensions of the Py sample used to obtain the hysteresis loop shown in Fig. 5 are 100 nm × 2.2 mm × 2.8 mm, which give a volume of 6.16×10^{-7} cm^3. Now considering that the saturation magnetization of Py is around 1 T or 800 emu/cm^3, the expected magnetic moment should be 4.9×10^{-4} emu. As observed in Fig. 5, the value of the magnetic saturation is slightly above 5×10^{-4} emu, which agrees with our estimation of the magnetic moment. The square shape of the magnetization curve and the very low coercive field indicate the presence of a well defined uniaxial anisotropy of the film. As it was expected, the coercive field of the FeNi layer is below 10 Oe. On the other hand Fig. 5b) shows the hysteresis loop along the hard axis of the FeNi film. As expected, a linear dependence of the magnetization and the lack of coercive field in the hysteresis loop was observed.

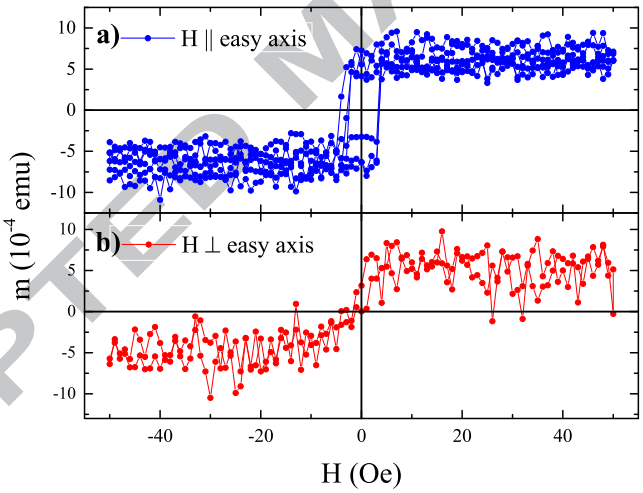

Figure 5: Magnetization curves of a 100 nm-thickness thin film of $Fe_{19}Ni_{81}$. The magnetic field was applied (a) parallel to the in-plane easy axis and (b) perpendicular to the easy axis. The diamagnetic signal arising from the sample holder was corrected through a linear fitting of the data.

The magnetization curves of the FeNi thin film evidence the relatively high sensitivity of our home-made vibrating sample magnetometer ($\sim 2 \times 10^{-4}$ emu) as a result of the pick-up coils optimization through numerical simulations.

4. Conclusions

In conclusion, we have been able to implement a vibrating sample magnetometer with a sensitivity of $\sim 2 \times 10^{-4}$ emu. The optimal physical dimensions and relative position between the pick-up coils in a Mallinson configuration were determined through numerical calculations of the sensitivity function based on the principle of reciprocity and the Biot-Savart law. Our results can be interpreted as a mechanism to determine the optimal dimension of the pick-up coils to enhance its sensitivity. Numerical simulations of the sensitivity function provided information about the performance of the detection mechanism in a multi-coil arrangement. Magnetization measurements in $Fe_{19}Ni_{81}$ confirmed that our magnetometer has an enhanced performance and is able to detect the magnetic moment of permalloy thin films of 100-nm thickness and also to identify interesting phenomena such as the presence of magnetic anisotropies.

The authors would like to thank V. Quinde and J. Pajuelo for their extraordinary technical support and A. Butera for the critical reading of the manuscript. This work was financially supported by the Programa Nacional de Innovación para la Competitividad y Productividad, Innóvate Perú, research project INNOVATE C.389-PNICP-PIBA-2014 and partially supported by the INNOVATE C.128-PNICP-PIAP-2014 of the Production Ministry of Peru.

References

[1] S. Foner, Versatile and Sensitive Vibrating Sample Magnetometer, Review of Scientific Instruments 30 (7) (1959) 548–557. doi:10.1063/1.1716679.

[2] E. E. Bragg, M. S. Seehra, Analysis of induced EMF in vibrating-sample magnetometers, Journal of Physics E: Scientific Instruments 9 (2001) 216–223. doi:10.1088/0022-3735/9/3/020.

[3] A. Zieba, S. Foner, Detection coil, sensitivity function, and sample ge-

ometry effects for vibrating sample magnetometers, Review of Scientific Instruments 53 (9) (1982) 1344–1354. doi:10.1063/1.1137182.

[4] S. Foner, Further improvements in vibrating sample magnetometer sensitivity, Review of Scientific Instruments 46 (10) (1975) 1425. doi:10.1063/1.1134021.

[5] J. Mallinson, Magnetometer Coils and Reciprocity, Journal of Applied Physics 37 (6) (1966) 2514–2515. doi:10.1063/1.1708848.

[6] J. A. Gerber, W. L. Burmester, D. J. Sellmyer, Simple vibrating sample magnetometer, Review of Scientific Instruments 53 (5) (1982) 691–693. doi:10.1063/1.1137043.

[7] W. Burgei, M. J. Pechan, H. Jaeger, A simple vibrating sample magnetometer for use in a materials physics course, American Journal of Physics 71 (8) (2003) 825. doi:10.1119/1.1572149.

[8] N. Hosseini, S. Khiabani, F. Sarreshtedari, M. Fardmanesh, Optimized design and implementation of low-cost, sensitive and versatile Vibrating Sample Magnetometer, in: 20th Iranian Conference on Electrical Engineering (ICEE2012), IEEE, 2012, pp. 202–205. doi:10.1109/IranianCEE.2012.6292353.

[9] T. M. El-Alaily, M. K. El-Nimr, S. A. Saafan, M. M. Kamel, T. M. Meaz, A. S. T., Construction and calibration of a low cost and fully automated vibrating sample magnetometer, Journal of Magnetism and Magnetic Materials 386 (5) (2015) 25–30. doi:10.1016/j.jmmm.2015.03.051.

[10] Core Team, R: A Language and Environment for Statistical Computing, Python: A dynamic, open source programming language (2014).
URL http://www.python.org/

[11] G. J. Bowden, Detection coil systems for vibrating sample magnetometers, Journal of Physics E: Scientific Instruments 5 (11) (1972) 1115. doi:10.1088/0022-3735/5/11/025.

[12] X. Xu, A. Sun, X. Jin, H. Fan, X. Yao, Method for calculating the induced voltage in a vibrating sample magnetometer detection coil system, Review of Scientific Instruments 67 (11) (1996) 3914–3923. doi:10.1063/1.1147292.

Highlights of the manuscript entitled

"Detection of magnetic moment in thin films with a home-made vibrating sample magnetometer."

The main contributions and highlights of this research are:

1) The optimization of the pick-up coils through numerical simulation based on the Biot-Savart law combined with the principle of reciprocity in electromagnetism.

2) The implementation of a home-made vibrating sample magnetometer with enhanced sensitivity ~ 2 x 10^{-4} emu.

3) The observation of in-plane magnetic anisotropies of thin films with a home-made VSM.